

Synthesis of Cellulose–Polylactic Acid Microcapsule as a Delivery Agent of Rifampicin

Suripto Dwi Yuwono^{1*}, Ridho Nahrowi¹, Andi Setiawan¹, Ni Luh Gede Ratna Juliasih¹, Irza Sukmana², Wasinton Simajuntak¹, Sutopo Hadi^{1*}

¹Department of Chemistry, Faculty of Mathematics and Natural Sciences, Universitas Lampung, Bandar Lampung, 35145, Indonesia

²Department of Mechanical Engineering, Faculty of Engineering, Universitas Lampung, Bandar Lampung, 35145, Indonesia

*Corresponding author: suripto.dwi@fmipa.unila.ac.id, sutopo.hadi@fmipa.unila.ac.id

Abstract

In medicinal field, delivery agent is a very important substance to improve the efficiency of drug used by improving the stability and preventing the degradation of drug during the medical treatment. Due to these important roles of the drug delivery agent, the search of effective agent is continuously in progress. In this respect, this current research was carried out to synthesize cellulose–polylactic acid (cellulose-PLA), as a potential delivery agent of rifampicin for the curing of tuberculosis. Cellulose was isolated from cassava bagasse, while PLA was obtained from commercial supplier. The two raw materials were used to synthesize cellulose–PLA in 3.5% HCl as solvent under magnetic stirring. The product obtained was then characterized by Fourier-Transform Infrared spectroscopy (FTIR), Particle-Size Analysis (PSA), and Scanning Electron Microscopy (SEM). The FT-IR result showed the presence of hydroxy (3446 to 3429 cm⁻¹) and carbonyl (1757 to 1759 cm⁻¹), confirming the formation new bond between cellulose and PLA. The PSA characterization displays a particle-sizes of PLA are in the range of 960–92780 nm, while cellulose–PLA are in the range of 100–17730 nm demonstrating that cellulose-PLA combined to form more compact structures. The results of SEM analysis indicate the distinct feature of cellulose-PLA, and combination of the features in the cellulose and PLA image. The results of the dissolution test carried out two different concentrations of rifampicin revealed that the optimum dissolution (8.42%) was achieved with cellulose–PLA of 0.3%, dissolution time of 12 h, and pH of 7.4.

Keywords

Cellulose, Cellulose-PLA, Dissolution Test, Polylactic Acid

Received: 21 January 2022, Accepted: 5 May 2022

<https://doi.org/10.26554/sti.2022.7.3.263-268>

1. INTRODUCTION

Aside from the human immunodeficiency virus, tuberculosis (TB) is one of the leading causes of death worldwide. In 2014, relatively 9.6 million new TB cases were recorded globally. Besides, approximately 1.5 million deaths have been recorded as a result of this disease (World Health Organization, 2016). One of the causes of the high death rate is TB cycle irregularity (Patel et al., 2013). However, continuous TB treatment leads to resistance to the antibiotic drugs administered. In addition, inappropriate administration of drugs leads to increased bacterial survival in host cells (Patel et al., 2013). Therefore, an innovation to reduce the death caused by this disease is urgently required.

Besides, for relatively 20 years, nanomaterial has been developed worldwide due to the wide range of applications, especially in the pharmaceutical field, owing to its numerous advantages. This is based on the fact that the nanomaterial design adapts to individual drug requirements. It serves as a controlled

release of drug encapsulation, enhances therapeutic efficacy, and reduces side effects (Amirah et al., 2014; Miricescu et al., 2019). The commonly used nanomaterials such as cellulose are natural polymers that are abundant in nature. Cellulose is a polysaccharide used in various applications due to its advantages, such as being non-toxic and renewable, and affordable processing cost (Guo et al., 2012). In addition, cellulose is a strong and rigid polymer that has a high potential to be used as a biopolymer reinforcing agent such as polylactic acid (PLA) (Rahman et al., 2014). Fortunately, PLA serves as a drug release because it is a biodegradable polymer that in vitro has good biocompatibility and bio-absorbability (Dev et al., 2010). Moreover, it has an aliphatic polyester structure (Guo et al., 2012). The active component of the drug bound to the PLA molecule is highly resistant to degradation, thereby improving its effectiveness (Kadian, 2018).

This led to the synthesis of cellulose–PLA, used in the encapsulation of rifampicin. The steps performed during the process included micro PLA, cellulose–PLA, and microcapsule

syntheses using rifampicin drug. Furthermore, FTIR, SEM, and dissolution test analyses as well as PSA were conducted.

2. EXPERIMENTAL SECTION

2.1 Materials

The materials utilized comprise PLA, hydrochloric acid, and chloroform obtained from Merck & Co (NJ, USA). Cellulose was extracted from cassava bagasse through delignification and applied without further treatment. Rifampicin was obtained from a local drug store and was used as purchased.

2.2 Synthesis of Micro PLA

The synthesis of micro PLA was conducted by dissolving 5 g of PLA in 50 mL of chloroform. The solution was stirred with a magnetic stirrer for 4 h. Furthermore, 50 mL of ethanol was added, and the solution was stirred using a magnetic stirrer (Stuart Magnetic Stirrer, China) for another 4 h. The solution was evaporated with a rotary evaporator (Buchi Rotary Evaporator, Switzerland) until only a small amount of solvent was left. Subsequently, 25 mL of distilled water was added and evaporated to get rid of the organic solvent. Finally, the micro PLA obtained was freeze-dried (ScanVac-Freeze dryers, Denmark).

2.3 Synthesis of Cellulose-PLA

The synthesis of cellulose-PLA was carried out by combining several methods reported in various studies (Dev et al., 2010; Jeevitha and Kanchana, 2014). Firstly, 1 g of cellulose was suspended in 50 mL HCl 3.5 M and stirred with a magnetic stirrer for 2 h at 50°C. Secondly, 5 g of PLA was dissolved in 50 mL of chloroform and stirred for 4 h. Subsequently, 50 mL of ethanol was added to the PLA solution, which was further mixed with the initially prepared cellulose suspension. The cellulose-PLA mixture was stirred for 4 h at room temperature and then transferred into a separating funnel. The upper layer, which comprises the chloroform, was removed using a bulb pipette, while the remaining cellulose-PLA was filtered with a filter paper and then freeze-dried. The sample was analyzed using FTIR (Agilent Carry 630, CA, USA), PSA (Fritsch, Germany), SEM (Zeiss Evo MA10, Germany).

2.4 Synthesis of Microcapsule

Meanwhile, approximately 0.65 g of cellulose-PLA was dissolved in 6 mL of chloroform. Consequently, rifampicin (0.0025 and 0.005 g) was added to the solution, followed by the addition of 50 mL polyvinyl alcohol 0.5%. It should be mentioned that the concentration of rifampicin used is much lower than the normally used dose for curing purpose, since the main objective of this study is to study the potential application of cellulose-PLA synthesized as delivery agent. The mixture was stirred for 1 h and dispersed in 250 mL of distilled water. Finally, the mixture was stirred for another 1 h and then filtered. The solid obtained was then dried for 24 h (Chang, 1984).

2.5 Slow Release Test

The slow-release test was carried out by dissolving 0.2 g of microcapsules into 500 mL of a buffer solution (pH 1.2 KCl-HCl buffer, and pH 7.4 phosphate buffer) with a pH of relatively 1.2 and 7.4. Therefore, for every 3 h interval, 5 mL of each solution, with triplicate sampling at pH of 1.2 and 7.4 was collected and diluted with 25 mL of buffer solution. The concentration was measured using a UV-Vis Shimadzu UV-245 Spectrophotometer (Japan) at a wavelength of 244 nm (Derakhshandeh and Soleymani, 2010; Ciobanu et al., 2013; Siqueira et al., 2010). The drug dissolution rate was further measured using the following formula (1)

$$\%D = \frac{M \times fp \times v \times \frac{1}{1,000,000}}{w} \times 100\% \quad (1)$$

Where Exp: % D (percent dissolution), M (concentration), fp (dilution factor), V (volume), W (mass of microcapsules used).

2.6 Characterizations

The IR spectra were recorded on KBr discs within the wavenumber range of 4000 to 400 cm^{-1} . The particle size distribution of PLA and cellulose-PLA were determined using the wet dispersion using water as solvent. SEM characterization was conducted on gold coated sample to increase the conductivity.

3. RESULTS AND DISCUSSION

3.1 Synthesis of Micro PLA and Cellulose-PLA

Besides, during the synthesis of micro PLA, mechanical treatment was adopted. Conversely, for the cellulose-PLA, a combination of mechanical and acid hydrolysis treatments was utilized. Micro PLA synthesis was carried out using a magnetic stirrer at a constant rotational speed. One advantage of the mechanical treatment is that the surface charge of the nanomaterial is equivalent to that of the raw material (Chang, 1984). Conversely, acid hydrolysis treatment was conducted using 3.5 M HCl solution. The acidic solution was used to break down the heterocyclic ether bond between the monosaccharide monomers (Siqueira et al., 2010; Laopaiboon et al., 2010).

The ionic strength of the HCl solution decreased the viscosity of cellulose, thereby reducing the size of the macromolecules (Czechowska-Biskup et al., 2007). Although, before mixing the PLA and cellulose solution, ethanol was added to the PLA solution, which acted as an emulsifier. It accumulated on the surface of the HCl and chloroform solution, thereby, causing ethanol to be adsorbed in the solution. In addition, ethanol also decreases the surface and interface strains of each solvent. Additionally, during the emulsion process, the molecules of cellulose and PLA were collided, thereby freely interacting with each other (Tadros, 2013). The collision frequency increased during the stirring process. Electromagnetic induction, which generated rotational motion at a constant angular velocity, enhanced the reaction rate of cellulose and PLA (Szajnar et al., 2014).

3.2 FTIR Analysis of Cellulose-PLA

FTIR analysis was carried out to determine the functional groups of materials synthesized. The FTIR spectra are shown in Figure 1. Figure 1(a) shows the absorption at 3446 cm^{-1} due to the presence of OH from cellulose. In addition, the absorption at 2900 and 1429 cm^{-1} indicates the C-H bond from the cellulose. These results show that pure cellulose was obtained through the delignification process. This was evidenced by the absence of absorption at 1170 and 1082 cm^{-1} . Meanwhile, the absorption of the pyranose ring originated from hemicellulose. In addition, the absence of an alkyl aryl ether bond at 1232 cm^{-1} indicated that no lignin was bound to the cellulose (Yang et al., 2007). This was proven by the absence of absorption at 1599 and 1511 cm^{-1} , indicating a phenylpropanoid ring of lignin (Adapa et al., 2011).

Figure 1(b) shows that the carbonyl group PLA is evident at 1757 cm^{-1} , CH_3 at 2999 cm^{-1} , and C-H at 2949 and 1458 cm^{-1} . The cellulose-PLA spectrum is shown in Figure 1(c). Furthermore, the presence of absorption at 1759 cm^{-1} indicates the presence of carbonyl derived from PLA. In addition, absorption at 3429 cm^{-1} implies that a hydroxyl group was derived from the cellulose. The presence of a hydroxy group is indicated by the presence of a band at relatively 3446 and 3429 cm^{-1} and carbonyl at approximately 1757 and 1759 cm^{-1} , thereby confirming the formation of a bond between the cellulose and PLA, while retaining their basic functional groups. Rahman et al. (2014) reported that the shift in wavenumbers was caused by the intermolecular hydrogen bonds between the cellulose and PLA.

3.3 PSA of Cellulose-PLA

Besides being used to detect particle size, PSA was also used to determine the effect of mechanical and acid hydrolysis treatments on micro-particle synthesis. The results of the effect of PSA on PLA and cellulose-PLA is shown in Figure 2. In accordance with Figure 2(a), PLA has 3 clusters of particles. The particle sizes in the first cluster range within 0.36 and $2.86\text{ }\mu\text{m}$, with a relative percentage of 11.75% . The second cluster overlapped with the third and the particle sizes ranging between 7.74 and $205\text{ }\mu\text{m}$, with a relative percentage of 87.18% . However, considering the cellulose-PLA (Figure 2(b)), the result showed that the sample size is much smaller while displaying a slightly narrower distribution. Based on the diagram, the particle size of the main cluster in the sample ranges within 8.30 to $37.86\text{ }\mu\text{m}$ with a relative percentage of 90.55% . This finding suggests that cellulose and PLA were combined to form a more compact material leading to the collapse of overlapping due to the mechanical and hydrolysis treatment during the preparation process. In respect to this, it was proven that a combination of mechanical and acid hydrolysis treatments improved the effectiveness of micro material synthesis. Mechanical treatment increased the frequency of polymer collisions in a solvent, thereby accelerating solvation. Acid hydrolysis treatment accelerated bonding by protonating polymer bonds.

In this study, it is evident that the particle size of the pre-

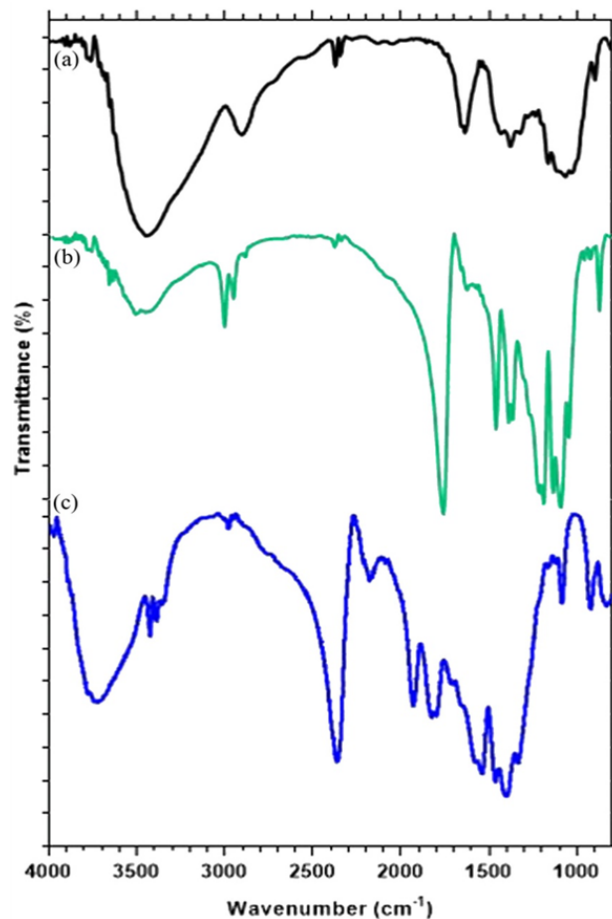


Figure 1. FTIR Spectra of (a) Cellulose, (b) PLA, (c) Cellulose-PLA

pared sample is within the micrometer (μm) range and significantly larger than the findings of the research carried out by Kumar et al. (2012), which reported that the preparation of co-ethyl cellulose-PLA had particle sizes within the nanometer (nm) range. These significantly different results were most likely realized due to the dissimilarities in the starting materials utilized.

3.4 SEM Analysis of Cellulose-PLA

SEM analysis was carried out to confirm the result of the cellulose-PLA synthesis morphologically, shown in Figure 3. Based on Figure 3(a), PLA has sheet morphology; this was due to the addition of chloroform. This solvent was diffused and adsorbed in the PLA 3-dimensional network, thereby breaking the cross-link. To confirm this notion, it was discovered that the density between PLA sheets was quite high. The chloroform disconnected the intermolecular, both physically and chemically. Figure 3(b) shows that the cellulose obtained through the delignification process has a rod-like structure. In addition, its intermolecular density was extremely high, indicating that the cellulose possesses a microcrystalline structure. Cellulose polymers possess uniform agglomeration due to the intramolecular

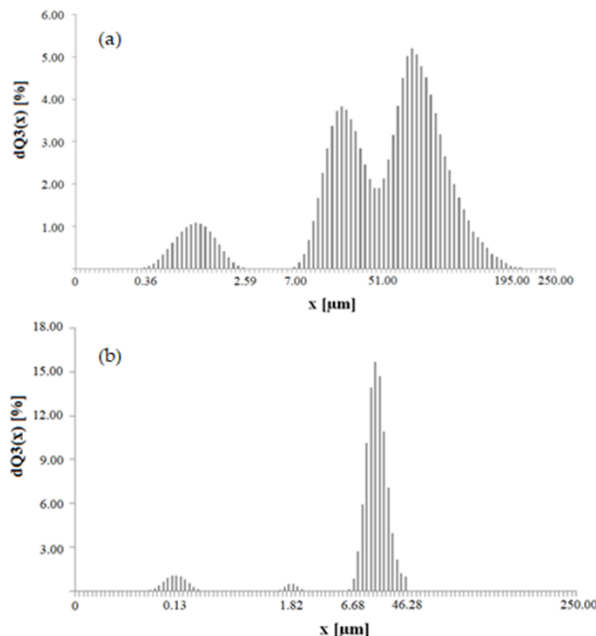


Figure 2. PSA Analysis (a) PLA, (b) Cellulose-PLA

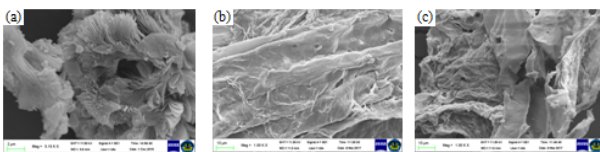


Figure 3. SEM Analysis (a) PLA, (b) Cellulose, (c) Cellulose-PLA

hydrogen bonds. Meanwhile, the cellulose microcrystal was composed of hundreds of agglomeration of cellulose nanofibrils with a rod-like structure (Rahman et al., 2014).

Based on Figure 3(c), the cellulose bounded into PLA particles has a smooth surface. The cellulose suspension process in the HCl was stirred in order to reduce agglomeration by hydrolyzing and breaking the intramolecular hydrogen bonds, thereby causing the inter-particle spacing to become more tenuous than that in Figure 3(b). It was also discovered that the density of the PLA particles attached to the cellulose was more tenuous than that in Figure 3(a) due to the HCl solvent hydrolyzed ether bonds on the PLA. The acid solution used was capable of hydrolyzing the long-chain cellulose in the amorphous part, thereby producing a crystalline structure. On the contrary, the crystalline part was resistant to acid attack (Khoo et al., 2016). The addition of cellulose caused the PLA structure to become more fragile than pure one (Sullivan et al., 2015), thereby increasing its dissolution ability in the body.

3.5 Dissolution Test

The dissolution test was carried out using rifampicin to determine the extent of its detachment from the micro material.

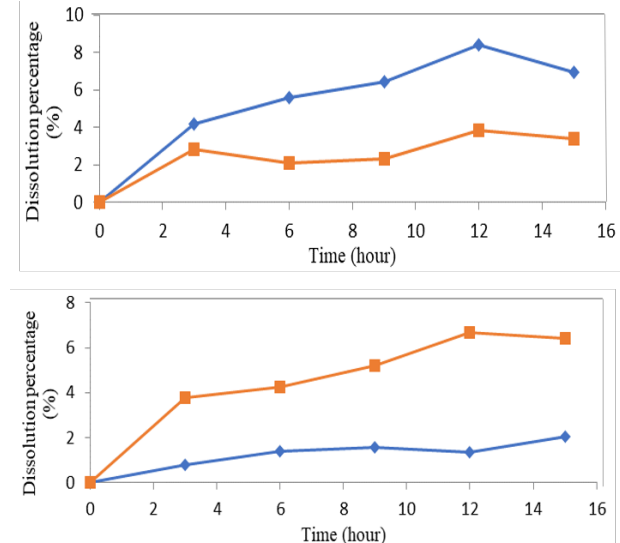


Figure 4. Dissolution Test of Rifampicin Concentration (a) 0.3% and (b) 0.6%

Rifampicin was selected because of its easy accessibility. The dissolution test was carried out at a pH of 1.2, which is regarded as a simulation of the stomach and intestinal pH of 7.4, carried out for 15 h. The dissolution test results are shown in Figure 4.

Figure 4(a) shows the percentage dissolution of PLA-cellulose-drug 0.3% at a pH of 7.4 and 1.2. The optimum time for drug dissolution at the same pH was 12 h. Furthermore, relatively 8.42% and 3.81% of the drugs were dissolved at a pH of 7.4, and 1.2 respectively. In addition, drug dissolution occurred more at a pH of 7.4 than 1.2. The percentage dissolution of PLA-cellulose-drug of 0.6%, is shown in Figure 4(b). The optimum time for drug dissolution at a pH of 7.4 was 15 h. In addition, approximately 2.03% of the drugs were dissolved. Conversely, the optimum time for drug dissolution at a pH of 1.2 was 12 h. Furthermore, approximately 6.69% of the drugs were dissolved. Therefore, the drug dissolution occurred more at pH 1.2 than 7.4.

An effective microcapsule used for TB treatment is cellulose-PLA-drug 0.3%. Conversely, several nanomaterial drugs were not degraded in the stomach, they were easily degraded in the lungs. The presence of a nanomaterial improved the effectiveness of the treatment and reduced the TB drug resistance caused by genetic mutations (Shakya et al., 2012). Based on the data in Figure 4, the optimum dissolution time for rifampicin is 12 h. This is consistent with the study carried out by Sarfaraz et al. (2010) which stated that after 12 h, approximately 69% to 91% of rifampicin was deformed. Amirah et al. (2014) reported that the optimum dissolution time for rifampin is 10 h. The dissolution rate on the first day was affected by several factors, such as diffusion through the cellulose-PLA channel. In addition, terminal carboxylic acids improved water absorption, thereby accelerating swelling and cellulose-PLA degradation

(Fonseca et al., 2002). The dissolution rate was also affected by the large surface area of the material (Nag et al., 2016).

4. CONCLUSIONS

In this research cellulose-PLA was successfully synthesized from cellulose isolated from cassava bagasse and commercial PLA. The formation of bond between the two starting materials was confirmed by FT-IR analysis as indicated by the presence of absorption bands at 3445 and 3429 cm⁻¹ associated with hydroxyl group and the band at 1757 and 1759cm⁻¹ associated with carbonyl group. PSA analysis indicated the reduction of particle size of cellulose-PLA compared to those of cellulose and PLA, confirming the formation of cellulose-PLA microcapsule. The formation of cellulose-PLA microcapsule was also confirmed by surface morphology of the samples as seen by SEM. the dissolution test carried out two different concentrations of ripamycin revealed that the optimum dissolution (8.42%) was achieved with cellulose-PLA of 0.3%, dissolution time of 12 h, and pH of 7.4.

5. ACKNOWLEDGMENT

The authors would like to thank to the Institute of Research and Community Services, Universitas Lampung that provided fund for this project to be undertaken through research program of Masterplan for Acceleration and Expansion of Indonesia's Economic Development, 2016. The authors would like to thank Enago (www.enago.com) for the English language proofread and review.

REFERENCES

- Adapa, P., L. Schonenau, T. Canam, and T. Dumonceaux (2011). Quantitative Analysis of Lignocellulosic Components of Non-Treated and Steam Exploded Barley, Canola, Oat and Wheat Straw using Fourier Transform Infrared Spectroscopy. *Journal of Agricultural Science and Technology*, **1**; 177
- Amirah, M., A. Amirul, and H. Wahab (2014). Formulation and Characterization of Rifampicin-Loaded P (3HB-co-4HB) Nanoparticles. *International Journal of Pharmacy and Pharmaceutical Sciences*, **6**(4); 140–6
- Chang, T. M. S. (1984). *Microencapsulation and Artificial Cells*. Springer
- Ciobanu, G., B. Ana-Maria, and C. Luca (2013). Nystatin-Loaded Cellulose Acetate/Hydroxyapatite Biocomposites. *Revista de Chimie*, **64**; 1426–1429
- Czechowska-Biskup, R., A. Wojtasz-Pajak, J. Sikorski, A. Henke, P. Ulański, and J. M. Rosiak (2007). Aqueous Solutions of Hydrochloric Acid as Simple Solvents of Chitosan for Viscosity-and Light-Scattering-based Molecular Weight Determination. *Polish Chitin Society*; 87–94
- Derakhshandeh, K. and M. Soleymani (2010). Formulation and In Vitro Evaluation of Nifedipine-Controlled Release Tablet: Influence of Combination of Hydrophylic and Hydophobic Matrix Forms. *Asian Journal of Pharmaceutics*, **4**(4); 185–193
- Dev, A., N. Binulal, A. Anitha, S. Nair, T. Furuike, H. Tamura, and R. Jayakumar (2010). Preparation of Poly (Lactic Acid)/Chitosan Nanoparticles for Anti-HIV Drug Delivery Applications. *Carbohydrate Polymers*, **80**(3); 833–838
- Fonseca, C., S. Simoes, and R. Gaspar (2002). Paclitaxel-Loaded PLGA Nanoparticles: Preparation, Physicochemical Characterization and In Vitro Anti-Tumoral Activity. *Journal of Controlled Release*, **83**(2); 273–286
- Guo, Y., X. Wang, X. Shu, Z. Shen, and R. C. Sun (2012). Self-Assembly and Paclitaxel Loading Capacity of Cellulose-Graft-Poly (Lactide) Nomicelles. *Journal of Agricultural and Food Chemistry*, **60**(15); 3900–3908
- Jeevitha, D. and A. Kanchana (2014). Evaluation of Chitosan/Poly(lactic acid) Nanoparticles for The Delivery of Piceatannol, an Anti-cancer Drug by Ionic Gelation Method. *International Journal of Chemical, Environmental and Biological Sciences*, **2**(1); 12–16
- Kadian, R. (2018). Nanoparticles: a Promising Drug Delivery Approach. *Asian Journal of Pharmaceutical and Clinical Research*, **11**(1); 30–5
- Khoo, R., H. Ismail, and W. Chow (2016). Thermal and Morphological Properties of Poly (Lactic Acid)/Nanocellulose Nanocomposites. *Procedia Chemistry*, **19**; 788–794
- Kumar, K. S., P. S. Kumar, V. Selvaraj, and M. Alagar (2012). Drug Delivery Studies of Gold Nanoparticles Decorated Polylactic Acid-Co-Ethyl Cellulose Nanocapsules. *International Journal of Nano and Biomaterials*, **4**(1); 12–20
- Laopaiboon, P., A. Thani, V. Leelavatcharamas, and L. Laopaiboon (2010). Acid Hydrolysis of Sugarcane Bagasse for Lactic Acid Production. *Bioresource Technology*, **101**(3); 1036–1043
- Miricescu, D., D. G. Balan, C. Radulescu, R. Radulescu, I. I. Stanescu, M. Mohora, B. Virgolici, A. Totan, and M. Greabu (2019). The Antioxidant Effects of PLGA-based Nanoparticles Loaded with Vitamin E in Rats Treated with Hypercaloric Diet. *Materiale Plastice*, **56**(2); 337
- Nag, M., V. Gajbhiye, P. Kesharwani, and N. K. Jain (2016). Transferrin Functionalized Chitosan-PEG Nanoparticles for Targeted Delivery of Paclitaxel to Cancer Cells. *Colloids and Surfaces B: Biointerfaces*, **148**; 363–370
- Patel, B. K., R. H. Parikh, and P. S. Aboti (2013). Development of Oral Sustained Release Rifampicin Loaded Chitosan Nanoparticles by Design of Experiment. *Journal of Drug Delivery*, **2013**
- Rahman, M. M., S. Afrin, P. Haque, M. Islam, M. S. Islam, and M. Gafur (2014). Preparation and Characterization of Jute Cellulose Crystals-Reinforced Poly (l-Lactic Acid) Biocomposite for Biomedical Applications. *International Journal of Chemical Engineering*, **2014**
- Sarfraz, M., D. Hiremath, and K. Chowdary (2010). Formulation and Characterization of Rifampicin Microcapsules. *Indian Journal of Pharmaceutical Sciences*, **72**(1); 101
- Shakya, N., G. Garg, B. Agrawal, and R. Kumar (2012).

- Chemotherapeutic Interventions Against Tuberculosis. *Pharmaceuticals*, **5**(7); 690–718
- Siqueira, G., S. Tapin-Lingua, J. Bras, D. da Silva Perez, and A. Dufresne (2010). Morphological Investigation of Nanoparticles Obtained from Combined Mechanical Shearing, and Enzymatic and Acid Hydrolysis of Sisal Fibers. *Cellulose*, **17**(6); 1147–1158
- Sullivan, E. M., R. J. Moon, and K. Kalaitzidou (2015). Processing and Characterization of Cellulose Nanocrystals/Polylactic Acid Nanocomposite Films. *Materials*, **8**(12); 8106–8116
- Szajnar, J., M. Stawarz, T. Wróbel, and W. Sebzda (2014). Influence of Selected Parameters of Continuous Casting in The Electromagnetic Field on The Distribution of Graphite and Properties of Grey Cast Iron. *Archives of Metallurgy and Materials*, **59**; 747–751
- Tadros, T. F. (2013). *Emulsion Formation and Stability*. John Wiley & Sons
- World Health Organization (2016). *Global Tuberculosis Report*. World Health Organization
- Yang, H., R. Yan, H. Chen, D. H. Lee, and C. Zheng (2007). Characteristics of Hemicellulose, Cellulose and Lignin Pyrolysis. *Fuel*, **86**(12-13); 1781–1788